

Experimental studies of headed stud shear connectors in UHPC Steel composite slabs

Xiao-Long Gao^{1a}, Jun-Yan Wang^{*1} and Jia-Bao Yan^{2b}

¹Key Laboratory of Advanced Civil Engineering Materials, Tongji University, Ministry of Education, Shanghai 201804, China

²School of Civil Engineering, Tianjin University, Tianjin 300350, China

(Received November 4, 2019, Revised January 6, 2020, Accepted January 21, 2020)

Abstract. Due to the high compressive and tensile strength of ultra-high performance concrete (UHPC), UHPC used in steel concrete composite structures provided thinner concrete layer compared to ordinary concrete. This led to the headed stud shear connectors embedded in UHPC had a low aspect ratio. In order to systematic investigate the effect of headed stud with low aspect ratio on the structural behaviors of steel UHPC composite structure s this paper firstly carried out a test program consisted of twelve push out specimens. The effects of stud height, aspect ratio and reinforcement bars in UHPC on the structural behaviors of headed studs were investigated. The push out test results shows that the increasing of stud height did not obviously influence the structural behaviors of headed studs and the aspect ratio of 2.16 was proved enough to take full advantage of the headed stud strength. Based on the test results, the equation considering the contribution of weld collar was modified to predict the shear strength of headed stud embedded in UHPC. The modified equation could accurately predict the shear strength of headed stud by comparing with the experimental results. On the basis of push out test results, bending tests consisted of three steel UHPC composite slabs were conducted to investigate the effect of shear connection degree on the structural behaviors of composite slabs. The bending test results revealed that the shear connection degree had a significantly influence on the failure modes and ultimate resistance of composite slabs and composite slab with connection degree of 96% in s hear span exhibited a ductile failure accompanied by the tensile yield of steel plate and crushing of UHPC. Finally, analytical model based on the failure mode of composite slabs was proposed to predict the ultimate resistance of steel UHPC composite slabs with different shear connection degrees at the interface.

Keywords: UHPC; headed stud; composite structure; push-out test; analytical model;

1. Introduction

Ultra-high performance concrete (UHPC) is an advanced cementitious composites consisting of high strength matrix and evenly embedded steel fibers (Kang *et al.* 2010, Yoo *et al.* 2015, Hoang and Fehling 2017, Prem *et al.* 2014). UHPC exhibits high compressive strength (>150MPa) (Luo *et al.* 2019) and tensile strength more than 7MPa (Wang and Guo 2018). Moreover, UHPC has high ductility, toughness and durability (Yoo *et al.* 2015). Due to the excellent mechanical properties and durability, UHPC has been increasingly used in structural components of civil infrastructure, e.g., repairing existing reinforced concrete (RC) members (Habel *et al.* 2007, Yin *et al.* 2017, Lampropoulos *et al.* 2016), precast UHPC girders, connection joints (Hamoda *et al.* 2017) and reinforcing the bridge deck (Shao *et al.* 2013, Dieng *et al.* 2013, Liu 2019).

Fiber-reinforced polymer (FRP) only can provide tensile resistance that has been widely used for reinforcing the structural elements (Lazreg *et al.* 2018, Zoubida *et al.* 2018, Hassaine *et al.* 2016, Hadji *et al.* 2016). Besides the tensile

strength, UHPC also could provide high compressive strength. UHPC used in the steel-concrete composite structure could take full advantage of the high tensile capacity of steel and the high compressive capacity of UHPC (Wang *et al.* 2019), as shown in Fig. 1. Recently, increasing studies have been performed to investigate the mechanical behaviours of steel-UHPC composite structures (Shao *et al.* 2013, Dieng *et al.* 2013, Zhang *et al.* 2016). Shao *et al.* (2013) proposed a composite deck system consisted of orthotropic steel deck and thin UHPC layer. UHPC applied in the in orthotropic steel deck system can enhance the stiffness of the deck plate and reduce the stress level in the steel decking, level in the steel decking, which can significantly increase the fatigue life of steel components. Wang *et al.* (2019) carried out a series of bending tests to investigate the effect of different connection types on the static structure behaviors of steel-UHPC composite beams, the connection types included headed studs, bonding using epoxy-based adhesive and UHPC directly cast on plate textures. Furthermore, UHPC was applied as the core material of SCS (steel-concrete-steel) sandwich beams to improve their structural behaviours. The novel steel-UHPC-steel sandwich beams were developed as containment buildings for third-generation nuclear power plant AP1000 (Lin *et al.* 2018).

For the steel-concrete composite structures, the composite behaviour was significantly influenced by shear connectors between steel and concrete (Liu *et al.* 2019).

*Corresponding author, Ph.D., Professor
E-mail: 14529@tongji.edu.cn

^a Ph.D. Student

^b Associate Professor

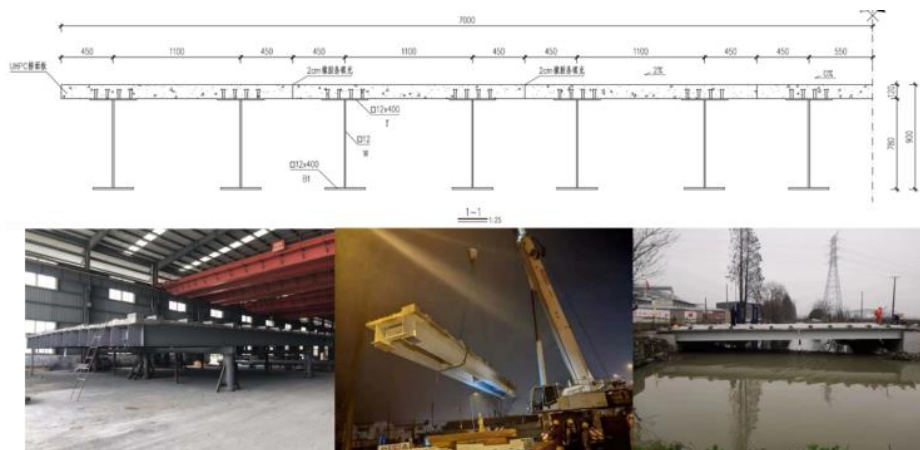


Fig. 1 Prefabricated steel-UHPC composite bridge girders in Ningbo, 2019

Some experimental studies have been conducted to investigate the behaviours of headed studs embedded in UHPC slabs in recent years (Kim *et al.* 2015, Cao *et al.* 2017, Wang *et al.* 2018, Wang *et al.* 2019). Kim *et al.* (2015) investigated the headed stud shear connectors embedded in UHPC slabs by push-out tests. Headed studs with diameters of 16 and 22 mm were used in the test program. The test results indicated that the stud aspect ratio of 3.1 and the cover thickness of 20 mm cannot lead to a reduction of stud shear strength and splitting crack at the UHPC slabs. Wang *et al.* (2018) experimentally studied the headed studs with large diameters of 22mm and 30mm. The test results proved that UHPC could resist the splitting force transferred by the headed studs and match well with the large headed studs. Based on the test results, Wang *et al.* (2018) proposed an empirical equation to predict the load-slip curve of headed stud embedded in UHPC. Wang *et al.* (2019) also investigated static behaviours of the group large headed stud embedded in UHPC slab. The research results revealed that the group headed studs led to a slight reduction of stud shear strength. Cao *et al.* (2017) conducted an experimental study on the static and fatigue behaviours of headed studs embedded in thin UHPC slabs with the stud diameter of 13 mm. The shear strength of headed stud was calculated according to the equation proposed by Doinghaus *et al.* (2003), which revealed that the equation considering the influence of weld collar at the end of headed stud could precisely predict the shear strength of headed stud embedded in UHPC. The previous experimental studies about the headed studs embedded in UHPC demonstrated that the strength of headed studs could be fully capitalized and no visible splitting cracks at the surface of UHPC slabs were observed after the push-out tests. These studies also revealed that the characteristic relative slips between steel and UHPC were all less than 6mm, which did not satisfy the ductility demand according to the code of Eurocode 4 (2005). Kim *et al.* (2015) thought that the elastic theory should be applied for the design of headed studs in steel-UHPC composite structures due to the ductility problem. Whereas, this conclusion was deduced according to the push-out test results, few experiments about the flexural behaviours of steel-UHPC composite structures with different headed stud spacings were

reported. In addition, previous push-out tests mainly investigated the effects of stud aspect ratio and UHPC slab thickness on the static behaviours of headed studs, few researchers studied the effect of stud height and reinforcement bars in the UHPC slabs.

In this paper, twelve push out test specimens and three steel UHPC composite slabs were used to investigate the structural behaviours of headed studs embedded in UHPC. The minimum aspect ratio of headed stud was low as 2.19 and the test results were complementary to the previous researches. Besides the variable of stud diameter and height, the effect of dense reinforcement bars in UHPC slabs on the static behaviours of headed stud was also investigated. The failure mode, damage areas of UHPC around headed studs, load slip curves were evaluated in this paper. The equations predicting the shear strength and load slips curve of headed stud were developed through modifying the previous equations. And the accuracies of the equations were validated against the reported test results. Moreover, four point flexural tests were conducted to investigate the effect of headed stud spacing on the structural behaviors of steel UHPC composite slabs. The failure modes, load deflection curves, relative slips at interface and strain distributions were evaluated. The analytical model was also developed to predict the ultimate resistance of steel UHPC composite slabs based on the bending tests.

2. Experiment program

2.1 Specimens and the set-up for push out test

Four groups of push-out specimens were fabricated and tested, as listed in Table 1, and each group included three specimens. The variables of the test program included stud diameter, stud height, stud aspect ratio and reinforcement bars in UHPC slab. Note that, the design codes of Eurocode 4 (2005) and AASHTO LRFD (2012) require the aspect ratio of at least 4 for headed stud to avoid the splitting failure of normal concrete. The previous push-out tests for headed stud embedded in UHPC indicated that the minimum stud aspect ratio of 2.3 can still lead to failure mode of stud fracture (Wang *et al.* 2019) and cover

thickness of 10 mm was enough for the steel-UHPC composite structures (Wang *et al.* 2017). In this paper, all the push-out test specimens were designed with a cover thickness of 15 mm. The specimen groups of D13H35 and D16H35 were designed with the same height of headed studs to check the influence of diameter. Headed studs in the specimen groups of D16H35 and D16H50 had a same diameter and different heights, which were used to study the effect of stud height. The influence of reinforcement bars on the static behaviour of headed stud was studied by comparing D16H35 and D16H35R.

The geometric dimensions of push-out specimens are shown in Fig. 2, which was designed based on the code of Eurocode 4 (2005). The steel I-beam with the section of 250mm×255mm×14mm×14mm was used in the specimens. Fig. 3 shows the fabrication process of the push-out test specimens. As shown in Fig. 2~3, the short beams were divided into two halves along the middle of the web. Two headed studs were welded on each flange face of the steel beams using a conventional stud-welding gun. The UHPC was then poured on the surface of steel beam flange horizontally, which was similar to the casting methods in the practical engineering. The two halves of the specimens were assembled together by six M24 high-tension bolts after curing under normal temperature condition for 28 days.

The set-up of push-out tests is shown in Fig. 4. The specimens were loaded by the electro servo-hydraulic pressure testing system with a load capacity of 3000 kN. Four linear variable differential transformers (LVDTs) were installed at the four corners of the steel beam to record the relative slips between UHPC slabs and steel beam. According to Eurocode 4 (2005), cycle load should be applied to stabilize the specimen and break the bond between steel beam and UHPC slabs. The cohesive stress between steel beam and UHPC slab was about 0.51MPa (Sun *et al.* 2017). The total bond force generated by the two surface of short steel beam was about 78.03kN. Thus, cyclic load with a value of 80kN was applied with a loading speed of 0.2kN/s. After the cyclic load, vertical loading was applied constantly and displacement loading with a rate of 0.15mm/min was used until the failure of specimen.

2.2 Specimens and set-up for bending test of steel-UHPC composite slabs

Three steel UHPC composite slabs with different stud spacing were fabricated and tested in four point bending. The details of composite slabs are shown in Fig. 5 and Table 2. Except for the stud spacing, all the composite slabs had the same dimensions with the overall depth of 60 mm, length of 1600 mm, width of 700 mm and casted with a net of Ø10 mm reinforcement bars. The spacing of reinforcement bars was 100 mm in transverse direction and 50mm in longitudinal direction, respectively.

Headed studs with diameter of 16mm and height of 35mm were welded on the steel plates. After that, the reinforcement mesh was put inside the wooden mold and the concrete cover with a thickness of 15mm was used. Then the fresh UHPC was poured into the mold. The specimens were cured at normal temperature for 28 days before the bending test.

Table 1 Details of push-out test specimens

Specimen	Thickness of UHPC slab (mm)	Stud shear connector			Reinforcement
		Diameter (mm)	Height (mm)	Aspect ratio	
D13H35-A~B	50	13	35	2.69	-
D16H35-A~B	50	16	35	2.19	-
D16H50-A~B	65	16	50	3.12	-
D16H35R-A~B	50	16	35	2.19	Φ10@100

Table 2 Details of composite slabs

Composite slab	L (mm)	L ₀ (mm)	b (mm)	a (mm)	ρ (%)
CS150	1600	1400	700	150	3.1
CS200	1600	1400	700	200	3.1
CS250	1600	1400	700	250	3.1

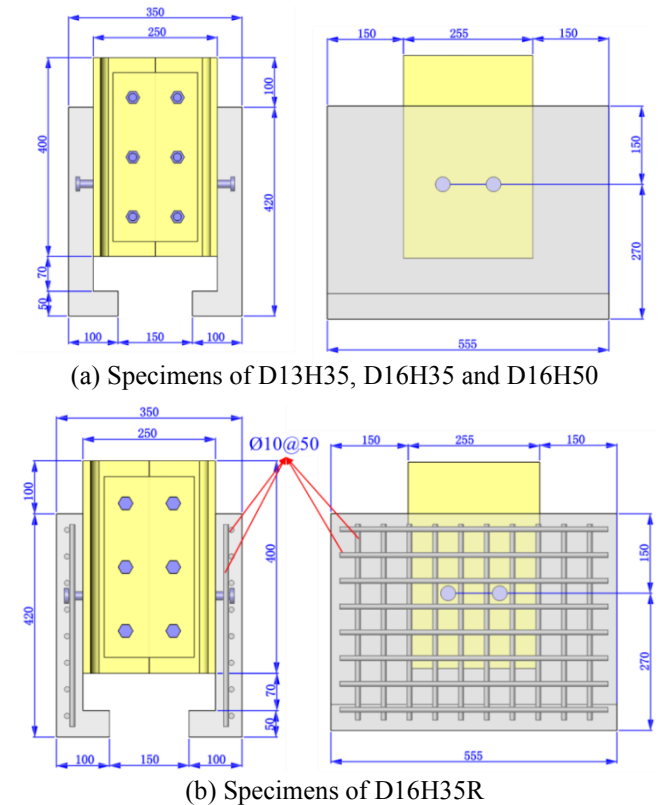


Fig. 2 Geometric dimensions of push-out test specimens (Unit: mm)

L and b denotes the length of composite slab specimen, respectively; L₀ denotes the clear span of composite slabs; a denotes the stud spacing; ρ denotes the longitudinal reinforcement ratio of composite slabs.

All the composite slabs were simply supported and tested under two point loading using hydraulic jack with a load capacity of 500 kN. The test set up is shown in Fig. 6. As shown in Fig. 6, the clear span was 1400 mm and the shear span was 500mm. The segmental loading method was



Fig. 3 Manufacture of push-out test specimens

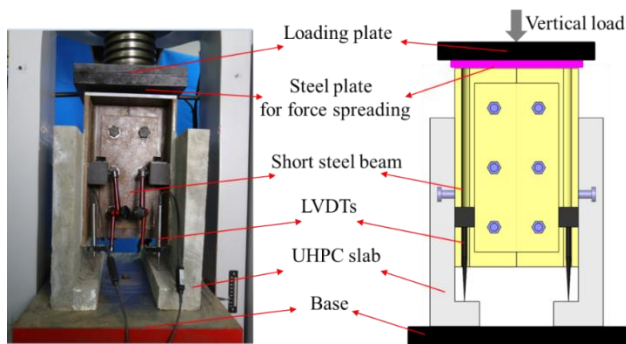


Fig. 4 Set-up for the push out test

Table 3 Mix proportions of premixed powder

Name	Cement	Silica fume	Ground filler	Quartz sand	Superplasticizer
Premixed powder	1	0.3	0.3	1.34	0.013

applied in the bending test program. Before the yield of composite slab, force control protocol with a rate of 20 kN/min was applied to the slabs according to the spreader beams. The load was increased at a step of 25kN and kept constant at each step to observe the cracks of UHPC layer. After the of the composite slab reached yield load, displacement control with a rate of 5mm/min was used.

Fig. 6(c) shows the detailed arrangement of measuring devices. As shown in Fig. 6(c), ten linear variable differential transformers (LVDTs) were installed at the bottom surface of composite slabs to monitor the vertical deflections of composite slabs. Two LVDTs were installed at the side surface of composite slabs to monitor the relative slips between steel plate and UHPC layer. Sixteen steel strain gauges and eighteen concrete strain gauges were placed at the surface of steel plates and UHPC layers.

2.3 Properties of UHPC, steel plate and headed stud

UHPC used in this paper was cured at room temperature without heat curing. It contained premixed powder, straight steel fibers (2.0% by volume) and water. The mix properties of premixed powder are listed in Table 3. The straight steel fibres coated with brass had a length of 13mm and a diameter of 0.2mm. The tensile strength of the steel fibres was specified for a minimum tensile strength of 2000MPa.

Table 4 Material properties.

	Thickness(mm)	f_{sy} (MPa)	f_{su} (MPa)	E_s (GPa)
Steel plate	10	345	355	206
Steel beam	12	357	462	201
Reinforcement	Diameter(mm)	f_y	f_u	E_{rs} (GPa)
		10	406/1.52%	
Headed stud	Diameter(mm)		f_{hu} (MPa)/	
		13,16	-	Cv
UHPC	f_{cu} (MPa)/Cov		f_{ct}	45
		133/3.3%	-	

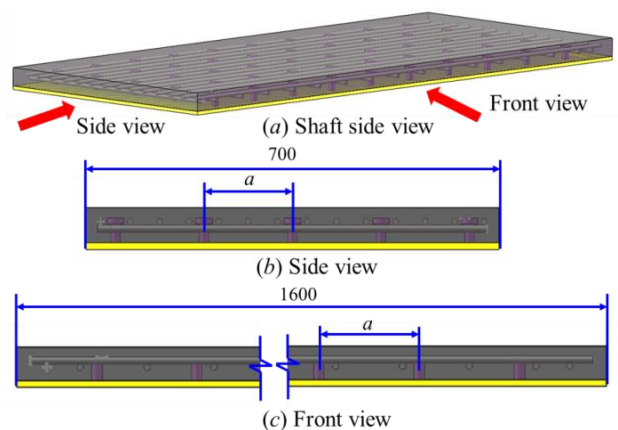
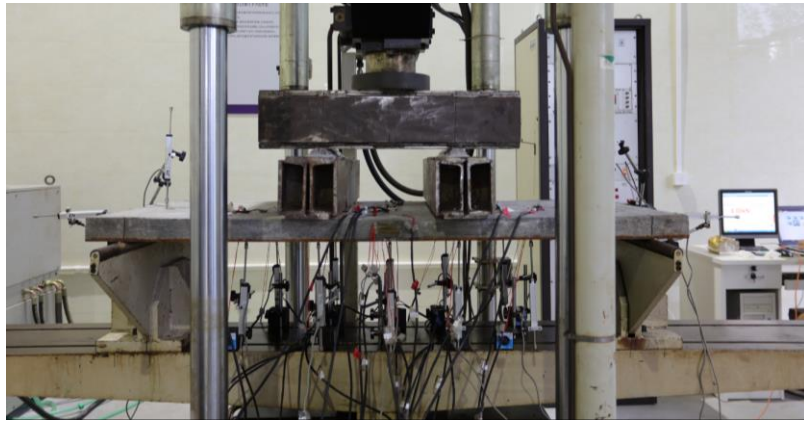
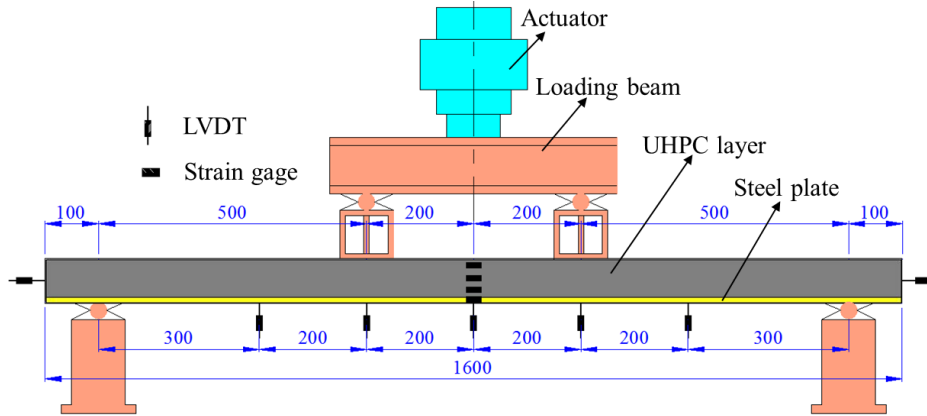


Fig. 5 Shape and dimensions of composite slab specimens

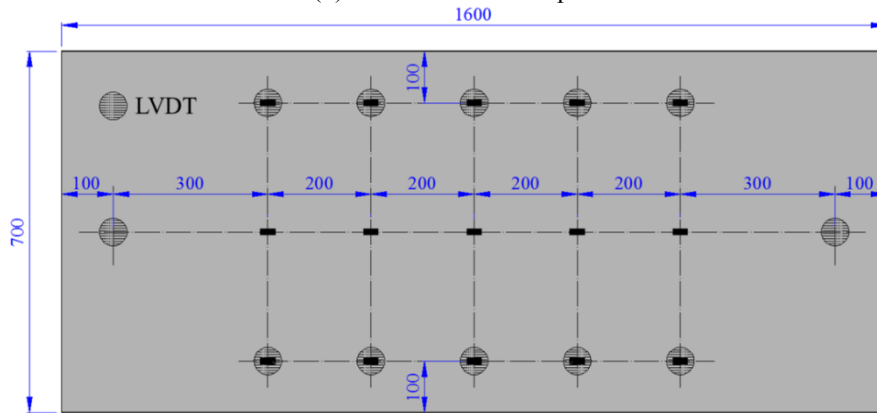
The compressive strength of UHPC was evaluated by 100mm cube compressive tests. The tensile properties of UHPC were tested using the dog-bone specimens with a section of 50mm×100mm (Wang et al. 2019). Three cube compressive specimens and three dog-bone tensile specimens for UHPC were casted and cured in the same condition of composite slabs and push-out specimens. The compressive and tensile mechanical properties of UHPC were tested after cured for 28 days. Fig. 7 shows the direct tensile stress-strain curves of UHPC. The 28-day compressive and tensile strength of UHPC are listed in Table 4. It shows that the average compressive and tensile strength were 133MPa and 8MPa, respectively. In addition, the elastic modulus of UHPC was 45GPa.



(a) Photo of test set-up



(b) Details of test set-up



(c) Layout of LVDTs and strain gages

Fig. 6 Test set-up for composite slabs

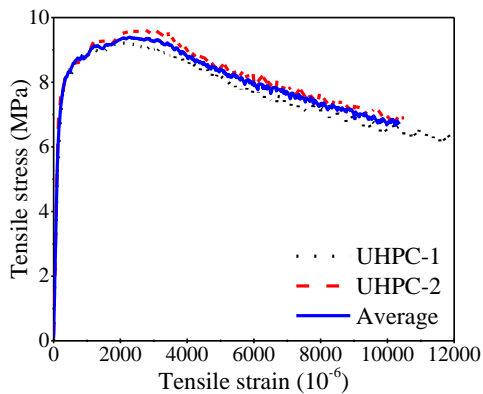


Fig. 7 Tensile stress-strain curves of UHPC

The steel plates for the steel-UHPC composite slabs and the steel I-beams were all made of Q345B. The mechanical properties of the steel plates and the steel beams provided by the manufacturer are shown in Table 4. Five headed studs with diameter of 16mm were tested under direct tensile test accordingly to the Chinese code of GB/T 10433-2002 (2002) to obtain its tensile strength. All the steel-UHPC composite slabs adopt Ø10mm reinforcing bars with ribs, and three tensile tests on the steel reinforcements were performed according to ASTM A370-13 (2013) to obtain their mechanical properties. The detailed mechanical properties are summarized in Table 4.

3. Test results and discussions

3.1 Results for push-out test

3.1.1 Failure mode and the damage area of UHPC slabs

Fig. 8 shows the failure mode of push-out test specimens, in which the surface of UHPC slabs and steel beams at failure are presented. As shown in Fig. 8, all the specimens failed in the mode of stud fracture and local concrete crushing in the inner side of headed studs. Moreover, headed studs in D16H35-C, D16H50-A and D13H35R-C all failed at the weld collar of stud and others failed at the shank of stud.

The minimum spacing of headed studs were generally determined by the crushing area of UHPC around headed stud. In order to obtain the dimensions of crushing areas around the headed studs, the photos of failure surface of UHPC slabs were imported into the software of CAD. Then those photos were scaled on the bias of the steel rule and the dimensions of damage areas in the UHPC slabs were marked, as shown in Fig. 8(a). The maximum width and height of crushing areas in the specimen group D13H35 were 28 mm and 29 mm, respectively, which were obviously less than the values of other specimen groups. This implied that the stud diameter had a significant impact on the crushing areas of UHPC. Comparing specimen group D16H35 with D16H50, decreasing the height of headed stud from 50 mm to 35 mm, the maximum width and the height of crushing areas increased by 4.6% and 9.3%, respectively. This revealed that the height of headed stud had negligible influence on the deformation of headed stud embedded in UHPC slab. Compare to the specimen group D16H35R, the maximum width and height of crushing areas decreased by 25.6% and 25.8%, respectively. This was because that reinforcement bars in UHPC slabs could enhance the strength and stiffness of UHPC around headed studs and the deformation of headed studs were limited, which may lead to the decreasing of crushing areas.

The above discussions show that there was some significant correlation between the dimensions of UHPC crushing areas and diameters of headed studs. The length and width of crushing area were directly related to the diameter of headed stud, as listed in Table 5. It shows that the maximum widths of UHPC crushing areas in each specimen group ranged from 2.2d to 2.7d and the maximum lengths ranged from 2.0d to 2.7d. Considering the safety and reliability of practical engineering, the minimum transverse spacing and the longitudinal spacing of headed studs shall not be less than 3.0d and 6.0d, respectively.

3.1.2 Shear strength and stiffness

Fig. 9 shows the load-slip curves of the push-out test specimens and Table 5 summarizes the shear strength and the corresponding relative slips, where P_{max} refers to the peak load obtained from load-slip curve and P_{stud} refers to the shear strength of single headed stud, which is calculated by dividing P_{max} by stud number. \overline{P}_{stud} refers to the average shear strength of headed studs in a specimen group. In addition, S_{max} refers to the relative slip related with the peak load, P_{max} . \overline{S}_{max} refers to the average slip of

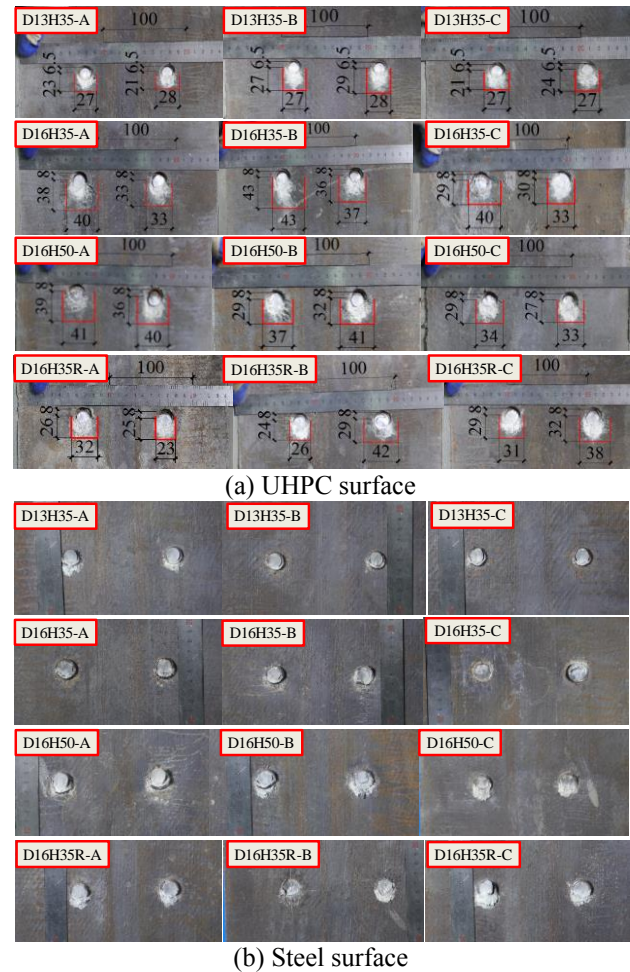


Fig. 8 Failure mode of push-out test specimens

headed studs in a specimen group. As can be seen from Fig. 9 and Table 5, larger diameter of headed stud led to higher shear strength and larger relative slip. As the diameter increased from 13mm to 16mm, the average shear strength, \overline{P}_{stud} , increased by 44.6% and the average relative slip, \overline{S}_{max} , increased by 64.8%. For specimens D16H35 and D16H50, as the height of headed stud increased from 35mm to 50mm, the average ultimate strength, \overline{P}_{stud} , increased only by 3.4%, whereas the average relative slip, \overline{S}_{max} , decreased by 0.8%, which reflected that the increasing of height of headed stud had negligible effect on the static behaviours of headed studs with diameter of 16mm and the aspect ratio of 2.16 was enough to take advantage of the strength of headed stud embedded in UHPC. For specimen D13H35R, the UHPC slabs were reinforced by reinforcement bars. The average shear strength, \overline{P}_{stud} , decreased by 5.6% and the average relative slip, \overline{S}_{max} , decreased by 5.5%. This is because that the stiffness of UHPC surrounding the headed stud are enhanced by the transverse reinforcement bars and the deformation of headed stud is constrained to some degree, which led to the decreasing of fracture surface area of headed studs.

As an important characteristic of headed studs, stiffness reflects the deformation capacity of headed studs, which is also an indicator to evaluate the performance of composite

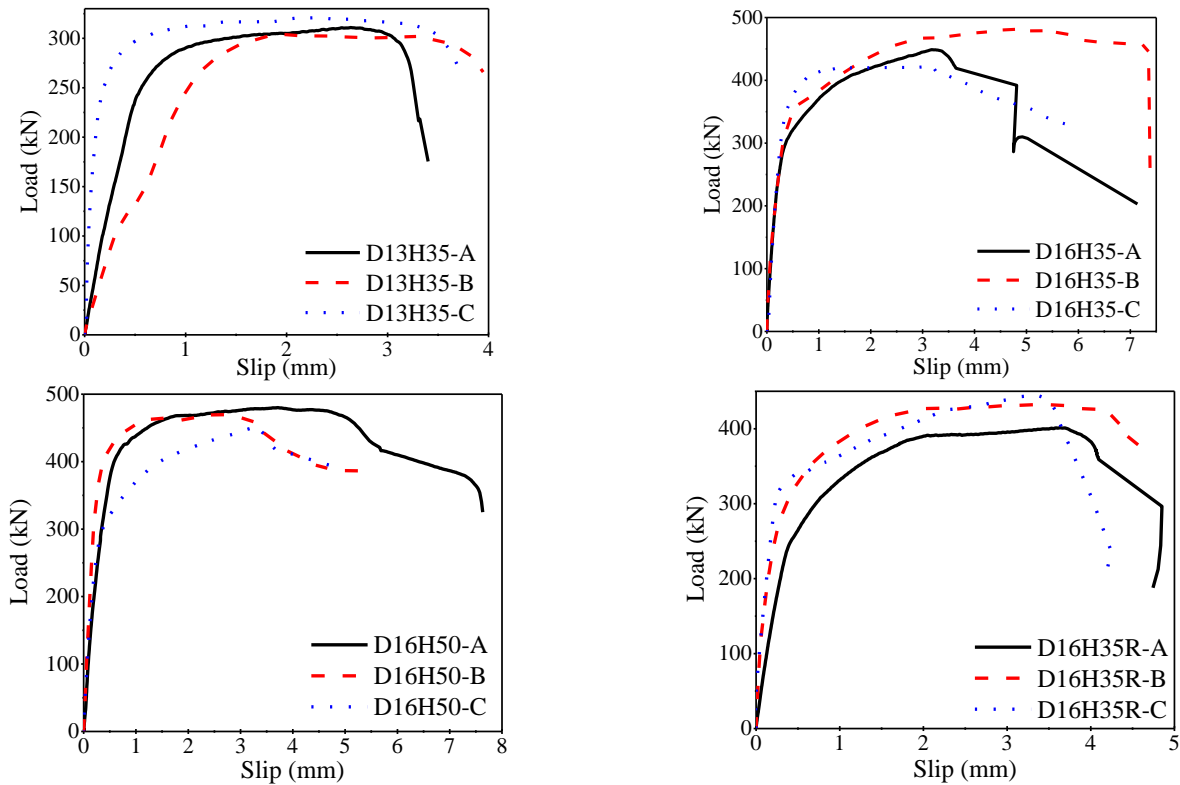


Fig. 9 Load-slip curves of push-out specimens

Table 5 Summary of push-out test results

Specimens	P_{max}	P_{stud}	\overline{P}_{stud}	S_{max}	\overline{S}_{max}	K_{stud}	\overline{K}_{stud}	Dimension of crushing area
A	310.9	77.7		2.63		122.8		HL:
D13H35 B	304.1	76.0	78.0	1.96	2.25	63.2	199.8	2.1d~2.2d
C	321.2	80.3		2.15		413.4		VL:1.6d~2.3d
A	448.8	112.2		3.17		178.2		HL:
D16H35 B	482.0	120.5	112.7	4.60	3.63	193.1	1219.2	2.1d~2.7d
C	422.6	105.6		3.07		286.3		VL:2.1d~2.7d
A	480.1	120.0		4.23		204.8		HL:
D16H50 B	469.9	117.4	116.5	3.12	3.60	372.2	2251.7	2.1d~2.6d
C	448.8	112.2		3.45		178.2		VL:1.7d~2.5d
A	401.4	100.3		3.63		119.4		HL:
D16H35R B	432.4	108.1	106.5	3.37	3.43	203.4	213.6	1.6d~2.6d
C	444.5	111.1		3.28		317.8		VL:1.5d~2.0d

* d denotes the diameter of headed stud; HL refers to the length in transverse direction; VL refers to the length in longitudinal direction.

structures in the serviceability limit state. According to Eurocode 4 (2005), the stud shear stiffness is defined as the secant stiffness at the point of 70% peak load in the load-slip curve. The shear stiffness of headed studs were calculated and listed in Table 5. As shown in Table 5, the shear stiffness increased significantly as the increasing of stud diameter. Whereas, increasing the height of studs or the arrangement of reinforcement bars in the UHPC slabs had neglected effect on the stiffness of headed studs.

Table 6 Summary of bending test of the composite slabs

Composite slab	Connection degree	P_u (kN)	$P_{u,Eq.(12)}$ (kN)	$\frac{P_u}{P_{u,Eq.(12)}}$	δ_u (mm)	ϵ_{y-s} (10^{-6})	ϵ_{u-s} (10^{-6})	Δ_{slip} (mm)
CS150	96%	320.2	351.6	0.91	27.94	3097	4025	0.82
CS200	58%	285.7	262.9	1.09	34.19	1542	4137	1.67
CS250	29%	174.9	160.1	1.09	27.58	1441	3408	1.84

3.2 Results for steel-UHPC composite slabs

3.2.1 Failure mode of UHPC slabs

The connection degrees of composite slabs were calculated by Eq. (1), and the calculation results were listed in Table 6.

$$\psi = nP_{stud}/F_{min} \quad (1)$$

where, n denotes the numbers of headed stud in the left or right span of composite slab; P_{stud} denotes the ultimate shear strength of headed stud obtained from the push-out test results. F_{min} denotes the minimum layer force between compression resistance of UHPC layer and tensile resistance of steel plate.

As shown in Table 6, Composite slab CS150 was designed with full connection between steel plate and UHPC layer. And the shear strength of headed studs in the shear span of composite slab CS150 was enough to ensure the transfer of shear force between steel plate and UHPC layer before the yield of steel plate. The composite slab behaved as a monolithic flexural member and no obvious separation at the interface between steel plate and UHPC slab was observed until the specimen reached ultimate resistance. The specimen failed in the yielding of steel plate and UHPC crushing, as shown in Fig. 10. Due to the strong

stud connection between steel plate and UHPC layer, the deformation of tensioned UHPC was effectively restricted by the steel plate and no crack was observed below a load of 272kN (about 85% of ultimate resistance). Slight interface cracks between the left load point and support were observed after a load of 156kN. Whereas, the widths of interface cracks hardly increased before the crushing of UHPC. Furthermore, after the ultimate resistance, as UHPC crushing occurred at the left load point, the vertical load center shifted to the left of composite slab, which led to a larger shear force at the left side of composite slab than that at the right side. After the ultimate resistance, obvious interfacial cracks were observed at the left shear span of composite slab. Lastly, some headed studs were fractured at the left shear span of composite slab when the vertical load dropped to 262kN (about 81% of the ultimate resistance).

For composite slabs of CS200 and CS250 designed with the connection degree of 58% and 29%, slight interfacial cracks between steel plates and UHPC layers were observed at a load of 75kN and 60kN, respectively. The separation was obvious between the loading point and the support as the increasing of vertical load. Flexure cracks with width of 0.04mm were observed below a load of 180kN (about 63% of ultimate resistance) and 100kN (about 57% of ultimate resistance), respectively. When the load reached about 80% of the ultimate resistance, some headed studs in the shear span were fractured and then the UHPC was crushed as the deformation of UHPC layer increased distinctly, as shown in Fig. 11(b) and (c). Furthermore, the depth of flexure cracks at the side surface of composite slabs increased as the increasing of stud spacing. When the composite slab reached ultimate resistance, the maximum flexural crack widths of specimens CS150, CS200 and CS250 were 0.24 mm, 0.5 mm and 0.66 mm, respectively.

3.2.2 Load-deflection curves and strain distribution

Fig. 12 shows the load versus mid-span deflection curves of the three composite slabs and Table 6 lists the ultimate resistance, P_u , and the corresponding midspan deflections, δ_u . It shows that the curves of composite slabs CS150 and CS200 had no differences below a load of 150 kN. For the composite slab CS150, the shear connections were enough to ensure the full use of strength for steel plate and UHPC. The ultimate resistance of composite slab CS150 was significantly higher than composite slabs of CS200 and CS250. As the connection degrees increased from 29% to 58% and 96%, the ultimate resistance of composite slabs increased by 63.4% and 83.1%, respectively. For composite slab CS200, as the lower shear connections between steel plate and UHPC layer, the flexure cracks were generated after a load of 180kN, the stiffness of composite slabs decreased rapidly compared to the curve of composite slab CS150. Furthermore, for the composite slab CS250 with connection degree of 29%, the stiffness began to decline after a load of about 40kN due to the poor connection between steel plate and UHPC layer.

Fig. 13 shows the strains of steel plates and UHPC layers at different loading levels, in which the solid lines represent the strains at the top surface of UHPC layers and the dashed lines represent strains at the bottom surface of steel plates. As illustrated in Fig. 13, for the composite slab

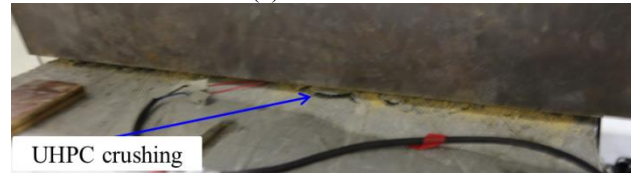
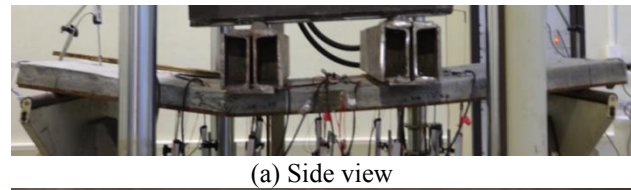


Fig. 10 Failure detail of CS150 under ultimate load

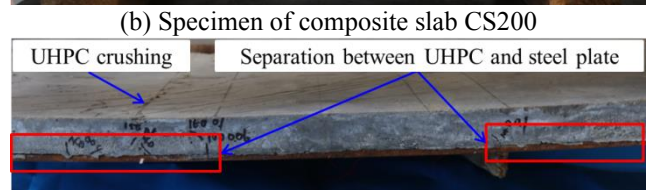
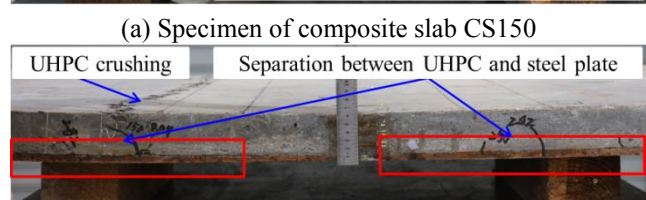
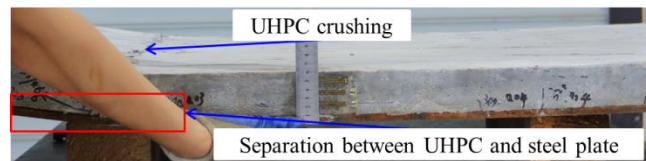


Fig. 11 Separation at the interface of UHPC and steel plate

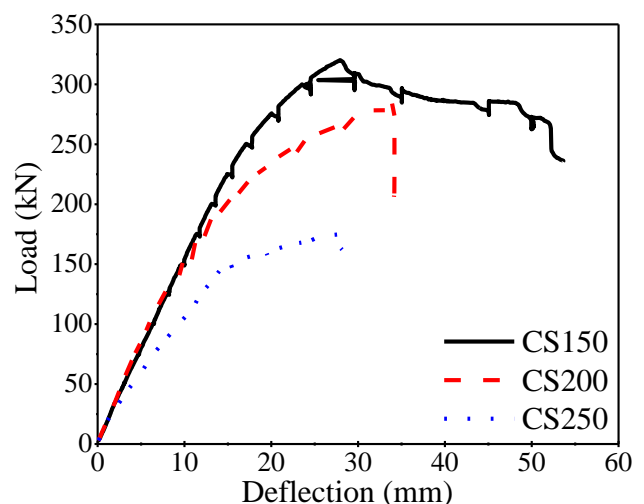
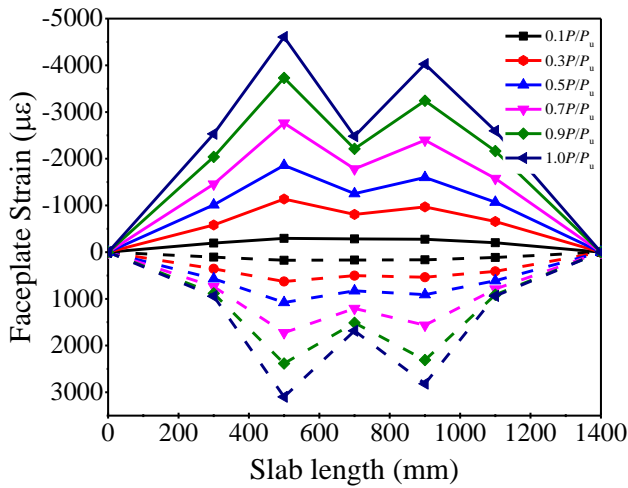
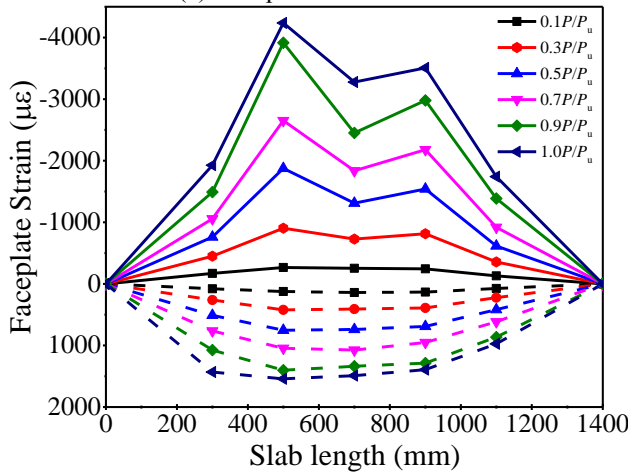


Fig. 12 Load-deflection curves of composite slabs

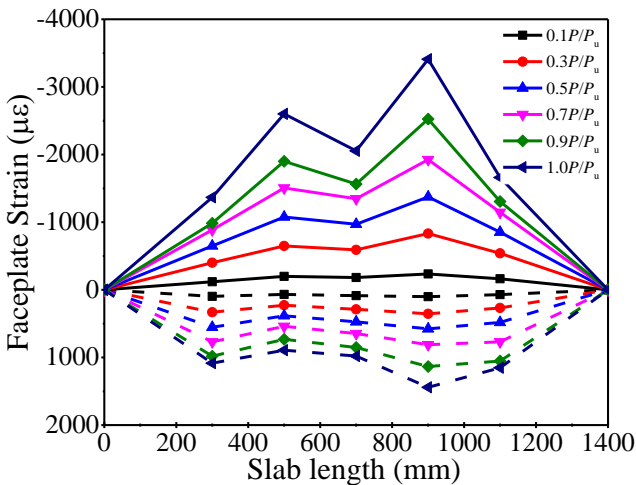
CS150, the strains of steel plate matched well with the strains of UHPC layer. Whereas, for composite slabs CS200 and CS250, the strains at the bottom surface of steel plate increased quickly than the strains at the top surface of UHPC. Table 6 summarizes the maximum steel strains and



(a) Composite slab CS150



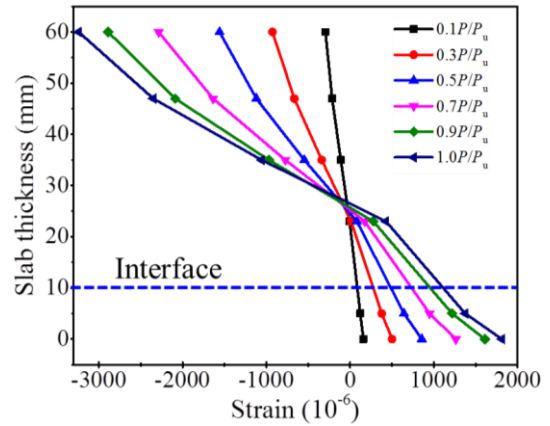
(b) Composite slab CS200



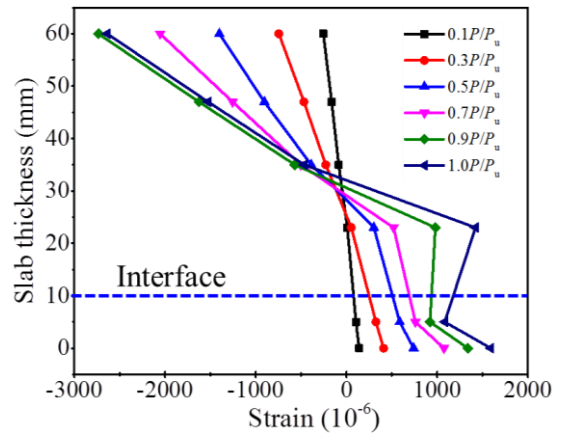
(c) Composite slab CS250

Fig. 13 Strain of UHPC and steel plate under different load levels

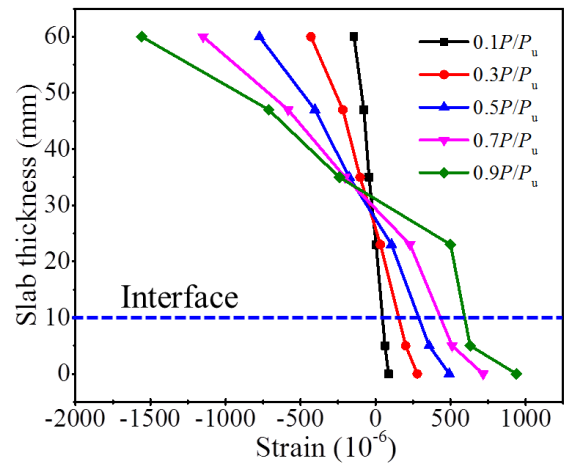
concrete strains when the specimens reached the ultimate resistance. As illustrated in Table 6, the steel plate strain of composite slab CS150 exceeded the yield strain of steel plate. Whereas, for composite slabs CS200 and CS250, the steel plate strain cannot exceeded the yield strain of steel plate. This was because the flexure stress can not be fully



(a) Composite slab CS150



(b) Composite slab CS200



(c) Composite slab CS250

Fig. 14 Strain for the mid-span section of composite slabs under different load levels

transferred to the steel plates due to the fracture of headed studs.

Fig. 14 shows the strain distribution at the mid-span section of composite slabs. As shown in Fig. 14, the composite slab CS150 exhibited flexural behavior consistent with an integrated steel plate and UHPC layer before the ultimate resistance. Whereas, for the composite slabs CS200 and CS250, the side strain was no longer planar after 70% of the ultimate resistance owing to the relative slip between UHPC layer and steel plate.

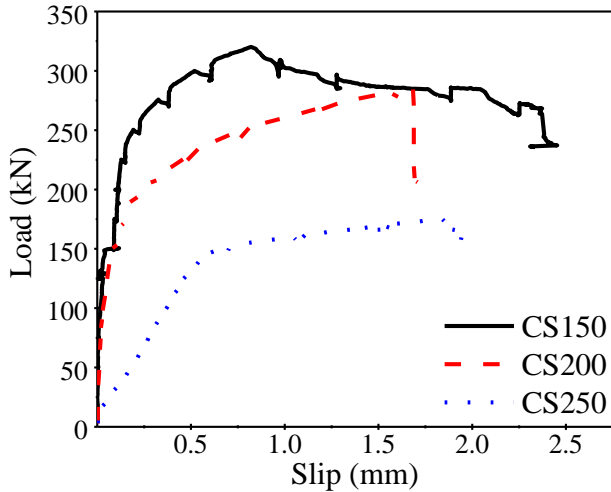


Fig. 15 Slip between the steel plates and UHPC layers

3.2.3 Load-slip curves

Fig. 15 shows the relative slips between steel plate and UHPC layer and Table 6 summarizes the slips when the specimens reached the ultimate resistance. As shown in Fig. 15, the relative slips for composite slabs CS150 and CS200 could be neglected before the yield load. And after the yield load, the slips increased slowly until the failed of specimens. For the specimen CS250, distinct slips were observed after a load of 20kN. The slips had a sudden increasing after the yield load due to the poor shear connection at the interface of steel plate and UHPC layer.

4. Evaluation of test results

4.1 Evaluation for push-out test results

4.1.1 Fitting for the load-slip curves

The load-slip curve is an important index to evaluate the mechanical behaviours of shear studs (Wang *et al.* 2019), which also determines the accuracy of numerical simulation results for the composite structures. Previous researchers have proposed several methods to predict the load-slip curves of headed studs (Ollgaard *et al.* 1971, Anand Cederwall 1996, Classen and Hegger 2017, Wang *et al.* 2019). However, most of these methods were inferred based on the test results of headed studs embedded in the normal concrete or the high strength concrete.

In order to verify the suitability of these formulas for headed studs embedded in UHPC slabs, Sun *et al.* (2017) modified the formula proposed by Ollgaard *et al.* (1971) according to the push-out test results of headed stud embedded in UHPC slab. The modified formula is expressed as following.

$$P = P_u (1 - e^{mS})^n \quad (2)$$

Where, P_u denotes the shear strength of headed studs; P denotes the shear load under different slips; S denotes the slips between steel beam and UHPC slabs (the unit is mm); $m=-3$, $n=0.5$, which were fitted on the basis of test results.

Wang *et al.* (2019) proposed an empirical equation considering the influence of stud diameter based on the push-out test results. The equation is expressed as following:

$$\frac{P}{P_u} = \frac{S / d_{stud}}{a + bS / d_{stud}} \quad (3)$$

where, d_{stud} denotes the diameter of studs; $a=0.006$, $b=1.02$, which denote the parameters fitted by the test results.

The empirical equations for headed stud embedded in UHPC slabs were all built based on the limited test results, which need further verification with more test data (Wang *et al.* 2019). In this paper, the push-out test results were used to fit the parameters in the above equations. The fitted equations are as following:

$$P = P_u (1 - e^{-1.79S})^{0.59} \quad (4)$$

$$\frac{P}{P_u} = \frac{S / d_{stud}}{0.016 + 0.92S / d_{stud}} \quad (5)$$

Fig. 16 compares the load-slip curves predicted by the above equations with curves obtained from push-out tests. As shown in Fig. 16, the equations fitted by Sun *et al.* (2017) and Wang *et al.* (2019) all overestimated the shear stiffness of headed studs. It may be caused by the difference elasticity modulus of UHPC (Sun *et al.* 2017). Correlation analysis was also conducted and Table 7 lists the analysis results. As shown in Fig.16 and Table 7, the Eq. (4) and Eq. (5) all could predict the load-slip curves reasonably. Moreover, the load-slip curves predicted by Eq. (5) could better match the test results as considering the diameter of headed studs in Eq. (5).

4.1.2 Shear bearing capacity of shear studs

Headed stud embedded in normal concrete failed in the surrounding concrete crushing or fracture of stud shank. The design formulas in codes were all built based on the two failure modes. The calculation formula in Eurocode 4 (2005) is defined as:

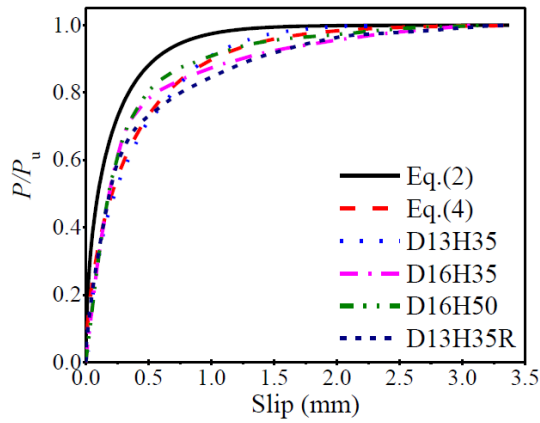
$$P_u = 0.29\alpha d^2 \sqrt{f_c E_c} / \gamma_v \leq 0.8A_{sc} f / \gamma_v \quad (6)$$

where, $\alpha = 0.2(h/d+1) \leq 1.0$; h and d denote the height and diameter of shear stud; f_c and E_c denote the compressive strength and the elasticity modulus of concrete; A_{sc} denotes the section area of stud; f denotes the tensile strength of stud; γ_v denotes the reduction factor, which is equal to 1.25.

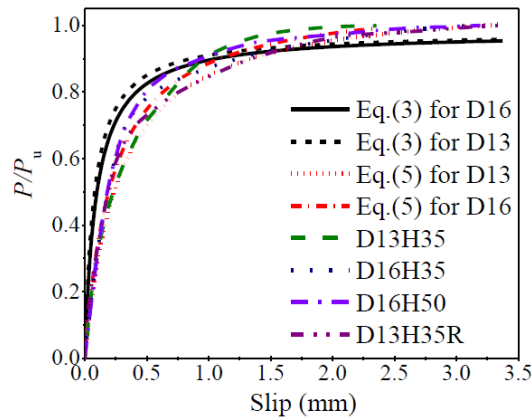
AASHTO LRFD (2012) defined the calculation formula of shear stud as following:

$$P_u = \phi 0.5 A_{sc} \sqrt{f_c E_c} \leq \phi A_{sc} f \quad (7)$$

Where, ϕ denotes the reduction factor, which is equal to 0.85.



(a) Predicted by Eq. (4)



(b) Predicted by Eq. (5)

Fig. 16 Comparison of load-slip curves between theoretical equations and test results

Table 7 Correlation analysis between test results and modified equations

Specimen	Correlation coefficients	
	Eq. (4)	Eq. (5)
D13H35	0.9993	0.9958
D16H35	0.9871	0.9899
D16H50	0.988	0.9861
D13H35	0.9933	0.9976
Mean	0.9919	0.9924

Previous studies (An and Cederwall 1996) revealed that the mechanical behaviours of headed stud embedded in high strength concrete were different from the headed stud embedded in normal concrete. The calculation methods for the shear strength of headed stud embedded in high strength shall consider the influence of weld collar. Based on pushout test results, Doinghaus *et al.* (2003) proposed the calculation formula of stud shear strength considering the weld dimensions as:

$$P_u = A_{sc}f + \eta f_c d_{wc} l_{wc} \quad (8)$$

where, d_{wc} denotes the diameter of shear stud weld; l_{wc} denotes the height of shear stud weld; η denotes the correction factor, which is equal to 1.5.

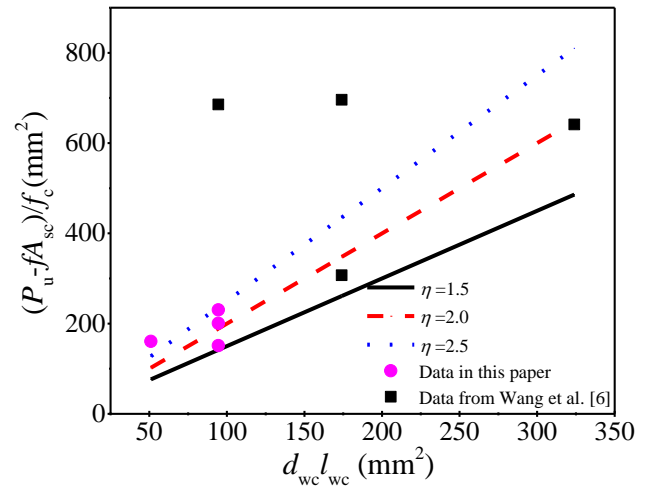


Fig. 17 comparison of different empirical factor η

Luo *et al.* (2016) suggested an empirical factor $\eta=2.5$ for headed stud embedded in high concrete with compressive strength range from 120MPa to 150MPa. Cao *et al.* (2019) verified the validity of the formula by the comparison of numerical simulation and experimental results. It concluded that for the headed studs in UHPC, the contribution of the weld collar should not be ignored. Otherwise, the calculation results may be too conservative.

Fig. 17 shows the relationship between the strength contributed by stud weld collar and the term related to the stud weld dimensions and UHPC compressive strength. Lines calculated by different empirical factors, η , were presented in Fig. 17. Table 8 lists the stud shear strength predicted by different methods. The reduction factors in Eq. (6) and Eq. (7) were set to be 1 for consistency. As can be seen from Fig. 17 and Table 8, $\eta=2.5$ may overestimate the studs with diameter of 16mm. $\eta=2.0$ appears acceptable with reasonable conservatism.

4.2 Evaluation for bending test results of composite slabs

The ultimate resistance of steel-UHPC composite slabs was accompanied by two failure modes: (1) the yield of steel plate and compressive crushing occurred at the top surface of UHPC layer; (2) the failure of headed studs in the shear span of composite slab and crushing occurred at the top surface of UHPC layer. Based on the characteristics of strain distribution at the mid-span section of composite slabs with different stud connection conditions, the resistance model for the composite slabs under ultimate resistance could be defined as Fig. 18. Furthermore, Fig. 18(b) represents section strain of composite slabs with full shear connection and Fig. 18(c) represents section strain of composite slabs with partial connection. It should be note that the thickness of UHPC is larger than the thickness of steel plate for the steel-UHPC composite slab, the neutral axis shall be located in the UHPC layer. As the height tensile strength of UHPC, UHPC in tensile zone also could resistance some tensile force, which is different with the conventional composite slabs, the tensile force in the concrete layer is resisted by the reinforcement.

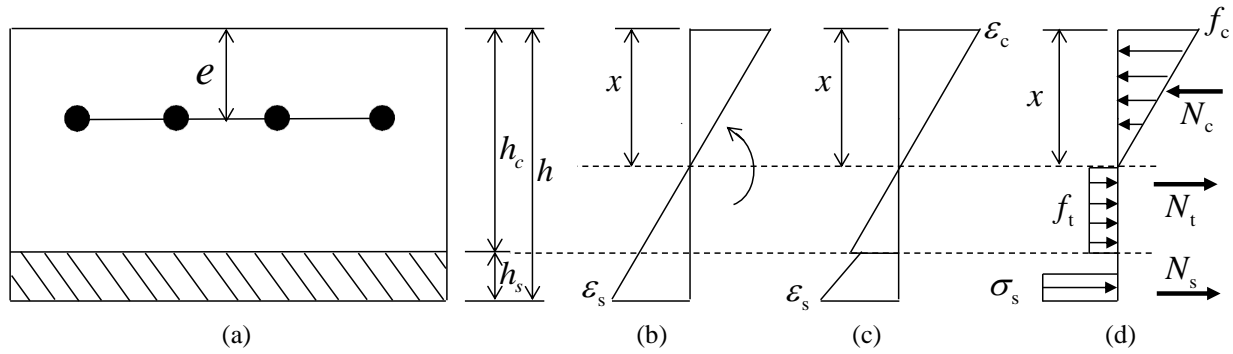


Fig. 18 Analysis model for ultimate load of composite slab

Table 8 Stud shear capacity predictions of different method versus test results

Specimen	\overline{P}_{stud}	$P_{Eucode}(\text{kN})$	$\frac{\overline{P}_{stud}}{\overline{P}_{Eucode}}$	$P_{AASHTO}(\text{kN})$	$\frac{\overline{P}_{stud}}{\overline{P}_{AASHTO}}$	$P_{Eq.(7)}(\text{kN})$	$\frac{\overline{P}_{stud}}{\overline{P}_{Eq.(7)}}$
D13H35	78.0	46.1	1.69	57.7	1.35	70.6	1.10
D16H35	112.8	69.9	1.61	87.4	1.29	111.3	1.01
D16H50	116.5	69.9	1.67	87.4	1.33	111.3	1.05
D16H35R	106.5	69.9	1.52	87.4	1.22	111.3	0.96
Mean			1.62		1.30		1.03

According to the analysis model, the force equilibrium equation can be defined as following:

$$N_c - N_t - F_d = 0 \quad (9)$$

$$0.5f_c bx - f_t b(h_c - x) - F_d = 0 \quad (10)$$

where, f_c and f_t denote the compressive and tensile stress of UHPC, respectively; b denotes the width of composite slab; h_c denotes the thickness of UHPC layer; h_s denotes the thickness of steel plate; F_d denotes the shear capacity provided by the headed studs in shear span, which should be less than the strength of steel plate, N_t , and the strength of UHPC layer, N_c .

The stress distribution in the steel plate is determined by the shear connection between steel plate and UHPC layer. In order to simply calculate the ultimate load of composite slabs, assuming the steel plates stress distribution as Fig. 18 (d). The relationship between F_d and N_s could be defined as:

$$F_d = N_s = f_y b x_e \quad (11)$$

The tension depth of steel plate, x_e , can be calculated according to Eq. (10) and The section-moment could be calculated as following.

$$M = \frac{1}{3} f_c b x^2 + \frac{1}{2} f_t b (h_c - x)^2 + F_d (h - x) - \frac{1}{2 f_y b} F_d^2 \quad (12)$$

The relationship between section moment and the vertical load could be defined as following:

$$P = \frac{2M}{a_0} \quad (13)$$

where, a_0 denotes the distance between support and loading point.

Table 6 lists the ultimate load of composite slabs calculated by Eq. (9)~(13) and verified with the test results, which resistance model calculated by Eq. (13) could well predict the ultimate flexural capacity of steel-UHPC composite slabs.

5. Conclusions

This paper reports the experimental and analytical studies on structural behaviours of headed studs embedded in UHPC. Push-out test consisted of twelve push-out specimens was carried out to investigate the influence of stud height, aspect ratio and dense reinforcement bars on the structural behaviours of headed studs. Based on the push-out test results, three steel-UHPC composite slabs were tested by four-point bending test to investigate the effect of stud spacing on the structural behaviours of steel-UHPC composite slab. The main conclusions are summarized as follows:

- All the push-out specimens failed in the mode of stud fracture and local concrete crushing in the inner side of headed studs. Increasing the height of headed stud did not obviously influence the structural behaviours of headed studs and the aspect ratio of 2.16 was proved enough to take full advantage of the headed stud strength.
- Detailed dimensions of UHPC crushing area around headed studs were measured and analyzed. The maximum length of crushing areas was 2.7 times diameter of headed stud. Considering the safety and reliability of steel-UHPC composite slabs in practical engineering, the minimum spacing of headed studs shall not be less than 6 times diameter in the curvature direction.
- The equations in current design codes all

underestimated the shear strength of headed stud embedded in the UHPC. A parametric study was conducted to investigate the effect of weld collar on shear strength of headed stud. And empirical equation considering the contribution of weld collar was modified to predict the shear strength of headed stud. Compared with the push-out test results, the modified equation could accurately predict the shear strength of headed stud embedded in UHPC.

- The shear connection degree in the shear span had a significant effect on the structural behaviours of steel-UHPC composite slabs. Composite slab CS150 with the connection degree of 96% exhibited a ductile failure accompanied by the tensile yield of steel plate and crushing of UHPC. Whereas, composite slabs CS200 and CS250 with connection degrees of 29% and 58%, respectively, exhibited brittleness failure as the shank failure of headed studs in the shear span. As the connection degrees increased from 29% to 58% and 96%, the ultimate resistance of composite slabs increased by 63.4% and 83.1%, respectively.

- Based on the two failure modes of steel-UHPC composite slab, analysis model considering shear connection degree at the interface of steel plate and UHPC was developed to predict the ultimate resistance of composite. The validation against the test and prediction results showed the reasonable and accuracy of the developed mode.

Acknowledgments

This work was supported by Zhejiang Communication Science and Technology Project [grant number 2019-GCKY-01], the National Nature Science Foundation of China [grant number 51609172] and the Shanghai Municipal Science and Technology Project [grant number 17DZ1204200]. The financial supports are greatly appreciated.

References

- AASHTO(2012), AASHTO LRFD Bridge Design Specifications, American Association of State Highway and Transportation Officials; Washington DC, United States.
- An, L. and Cederwall, K. (1996), "Push-out tests on studs in high strength and normal strength concrete", *J. Constr. Steel Res.*, **36**(1), 15-29. [https://doi.org/10.1016/0143-974X\(94\)00036-H](https://doi.org/10.1016/0143-974X(94)00036-H).
- ASTM A370-13 (2013), Standard Test Methods and Definitions for Mechanical Testing of Steel Products. ASTM International, 100 Barr Harbor Drive, PO Box C700, West Conshohocken, PA 19428-2949, United States.
- Cao, J.H., Shao, X.D., Deng, L. and Gan, Y.D. (2017), "Static and fatigue behavior of short-headed studs embedded in a thin ultrahigh-performance concrete layer", *J. Bridge Eng.*, **22**(5), 04017005. [https://doi.org/10.1061/\(ASCE\)BE.1943-5592.0001031](https://doi.org/10.1061/(ASCE)BE.1943-5592.0001031).
- Cao, J.H., Shao, X.D. (2019), "Finite element analysis of headed studs embedded in thin UHPC", *J. Constr. Steel Res.*, **161**(7), 355-368. <https://doi.org/10.1016/j.jcsr.2019.03.016>.
- Dieng, L., Marchand, P., Gomes, F., Terrier, C. and Toutlemonde, F. (2013), "Use of UHPFRC overlay to reduce stresses in orthotropic steel decks", *J. Constr. Steel Res.*, **89**(10), 30-41. <https://doi.org/10.1016/j.jcsr.2013.06.006>.
- Doinghaus, P., Goralski, C. and Will, N. (2003), "Design rules for composite structures with high performance steel and high performance concrete", International Conference on High Performance Materials in Bridges, Kona, HI, July.
- Eurocode 4(2005), Design of composite steel and concrete structures. Part 2: General rules for bridges, European Committee for Standardization; London, Britain.
- GB/T 10433-2002 (2002), Cheese head studs for arc stud welding, Inspection and Quarantine of the People's Republic of China; Beijing, Chinese. (in Chinese).
- Habel, K., Denarić, E. and Brühwiler, E. (2007), "Experimental investigation of composite ultra-high-performance fiber-reinforced concrete and conventional concrete members", *ACI Struct. J.*, **104**(1), 93-104. <http://orcid.org/0000-0002-2588-432X>.
- Hadji, L., Ait Amar Meziane, M., and Safa, A., (2018), "A new quasi-3D higher shear deformation theory for vibration of functionally graded carbon nanotube-reinforced composite beams resting on elastic foundation", *Struct. Eng. Mech.*, **66**(6), 771-781. <https://doi.org/10.12989/sem.2018.66.6.771>.
- Hadji, L., Hassaine Daouadji, T., Ait Amar Meziane, M., and Adda Bedia, E.A. (2016), "Analyze of the interfacial stress in reinforced concrete beams strengthened with externally bonded CFRP plate", *Steel. Compos. Struct.*, **20**(2), 413-429. <https://doi.org/10.12989/scs.2016.20.2.413>.
- Hamoda, A., Hossain, K.M.A., Sennah, K., Shoukry, M. and Mahmoud, Z. (2017), "Behaviour of composite high performance concrete slab on steel I-beams subjected to static hogging moment", *Eng. Struct.*, **140**(6), 51-65. <https://doi.org/10.1016/j.engstruct.2017.02.030>.
- Hassaine Daouadji, T., Hadji, L., Ait Amar Meziane, M., and Bekki, H., (2016), "Elastic analysis effect of adhesive layer characteristics in steel beam strengthened with a fiber-reinforced polymer plates", *Struct. Eng. Mech.*, **59**(1), 83-100. <https://doi.org/10.12989/sem.2016.59.1.083>.
- Hoang, A.L. and Fehling, E. (2017a), "A review and analysis of circular UHPC filled steel tube columns under axial loading", *Struct. Eng. Mech.*, **62**(4), 417-430. <https://doi.org/10.12989/sem.2017.63.3.371>.
- Hoang, A.L. and Fehling, E. (2017b), "Assessment of stress-strain model for UHPC confined by steel tube stub columns", *Struct. Eng. Mech.*, **63**(3), 371-384. <https://doi.org/10.12989/sem.2017.63.3.371>.
- Kang, S.T., Lee, Y., Park, Y.D. and Kim, J.K. (2010), "Tensile fracture properties of an Ultra High Performance Fiber Reinforced Concrete (UHPFRC) with steel fiber", *Compos. Struct.*, **92**(1), 61-71. <https://doi.org/10.1016/j.compstruct.2009.06.012>.
- Khelifa, Z., Hadji, L., Hassaine Daouadji, T. and Bourada, M., (2018), "Buckling response with stretching effect of carbon nanotube-reinforced composite beams resting on elastic foundation", *Struct. Eng. Mech.*, **67**(2), 125-130. <https://doi.org/10.12989/sem.2018.67.2.125>.
- Kim, J.S., Kwark, J., Joh, C., Yoo, S.W. and Lee, K.C. (2015), "Headed stud shear connector for thin ultrahigh-performance concrete bridge deck", *J. Constr. Steel Res.*, **108**(5), 23-30. <https://doi.org/10.1016/j.jcsr.2015.02.001>.
- Lampropoulos, A., Paschalis, S.A., Tsioulou, O. and Dritsos, S.E. (2016), "Strengthening of reinforced concrete beams using ultra high performance fibre reinforced concrete (UHPFRC)", *Eng. Struct.*, **106**(11), 370-384. <https://doi.org/10.1016/j.engstruct.2015.10.042>.
- Lin, Y.Z., Yan, J.C., Cao, Z.G., Zeng, X.Z., Fan, F. and Zou, C.Y. (2018), "Ultimate strength behaviour of S-UHPC-S and SCS sandwich beams under shear loads", *J. Constr. Steel Res.*, **149**(10), 195-206. <https://doi.org/10.1016/j.jcsr.2018.07.024>.
- Liu, Y.M., Zhang, Q.H., Bao, Y. and Bu, Y.Z. (2019), "Static and

- fatigue push-out tests of short headed shear studs embedded in Engineered Cementitious Composites (ECC)", *Eng. Struct.*, **182**(3), 29-38. <https://doi.org/10.1016/j.engstruct.2018.12.068>.
- Liu, Y.M., Zhang, Q.H., Meng, W.N., Bao, Y. and Bu, Y.Z. (2019), "Transverse fatigue behaviour of steel-UHPC composite deck with large-size U-ribs", *Eng. Struct.*, **180**(2), 370-384. <https://doi.org/10.1016/j.engstruct.2018.11.057>.
- Luo, J., Shao, X.D., Fan, W., Cao, J.H. and Deng, S.W. (2019), "Flexural cracking behavior and crack width predictions of composite (steel+UHPC) lightweight deck system", *Eng. Struct.*, **194**(1), 120-137. <https://doi.org/10.1016/j.engstruct.2019.05.018>.
- Luo, Y.B., Hoki, K., Hayashi, K. and Nakashima, M. (2016), "Behavior and strength of headed stud-SFRCC shear connection. II: Strength Evaluation", *J. Struct. Eng.*, **142**(2), 04015113. [https://doi.org/10.1061/\(ASCE\)ST.1943-541X.0001372](https://doi.org/10.1061/(ASCE)ST.1943-541X.0001372).
- Ollgaard, J.G., Slutter, R.G. and Fisher, J.W. (1971), "Shear strength of stud connectors in light weight and normal-weight concrete", *AISC. Eng. J.*, **8**(2), 55-64. <https://preserve.lehigh.edu/engr-civil-environmental-fritz-lab-reports/2010>.
- Prem, P. R., Verma, M., Ramachandra, M. A., Rajasankar, J. and Bharatkumar, B.H. (2017), "Numerical and theoretical modelling of low velocity impact on UHPC panels" , *Struct. Eng. Mech.*, **63**(2), 207-215. <https://doi.org/10.12989/sem.2017.63.2.207>.
- Shao, X.D., Yi, D., Huang, Z., Zhao, H., Chen, B. and Liu, M. (2013), "Basic performance of the composite deck system composed of orthotropic steel deck and ultrathin RPC layer", *J. Bridge. Eng.*, **18**(5), 417-428. [https://doi.org/10.1061/\(ASCE\)BE.1943-5592.0000348](https://doi.org/10.1061/(ASCE)BE.1943-5592.0000348).
- Sun, Q.L., Lu, X.Y., Nie, X., Han, Z.J. and Fan, J.S. (2017), "Experimental research on tensile and shear behaviour of the interface between non-steam-cured uhpc and steel plate structure", *Eng. Mech.*, **34**(9), 167-174.(in Chinese).
- Wang, J.Q., Qi, J.N., Tong, T., Xu, Q.Z. and Xiu, H.L. (2019), "Static behavior of large stud shear connectors in steel-UHPC composite structures", *Eng. Struct.*, **178**(1), 534-542. <https://doi.org/10.1016/j.engstruct.2018.07.058>.
- Wang, J.Q., Xu, Q.Z., Yao, Y.M., Qi, J.N. and Xiu, H.L. (2018), "Static behavior of grouped large headed stud-UHPC shear connectors in composite structures", *Compos. Struct.*, **206**(15), 202-214. <https://doi.org/10.1016/j.compstruct.2018.08.038>.
- Wang, J.Y., Gao, X.L. and Yan, J.B. (2019), "Behaviours of steel-fibre-reinforced ULCC slabs subject to concentrated loading", *Struct. Eng. Mech.*, **71**(4), 407-416. <https://doi.org/10.12989/sem.2019.71.4.407>.
- Wang, J.Y. and Guo, J.Y. (2018), "Damage investigation of ultra high performance concrete under direct tensile test using acoustic emission techniques", *Cem. Concr. Compos.*, **88**(4), 17-28. <https://doi.org/10.1016/j.cemconcomp.2018.01.007>.
- Wang, J.Y., Guo, J.Y., Jia, L.J., Chen, S.M. and Dong, Y. (2017), "Push-out tests of demountable headed stud shear connectors in steel-UHPC composite structures", *Compos. Struct.*, **170**(6), 69-79. <https://doi.org/10.1016/j.compstruct.2017.03.004>.
- Wang, Z., Nie, X., Fan, J.S., Lu, X.Y. and Ding, R. (2019), "Experimental and numerical investigation of the interfacial properties of non-steam-cured UHPC-steel composite beams", *Constr. Build. Mater.*, **195**(1), 323-39. <https://doi.org/10.1016/j.conbuildmat.2018.11.057>.
- Yin, H., Teo, W. and Shirai, K. (2017), "Experimental investigation on the behaviour of reinforced concrete slabs strengthened with ultra-high performance concrete", *Constr. Build. Mater.*, **155**(30), 463-474. <https://doi.org/10.1016/j.conbuildmat.2017.08.077>.
- Yoo, D.Y., Banthia, N., Kim, S.W. and Yoon Y.S. (2015), "Response of ultra-high-performance fiber reinforced concrete beams with continuous steel reinforcement subjected to low velocity impact loading", *Compos. Struct.*, **126**(8), 233-45. <https://doi.org/10.1016/j.compstruct.2015.02.058>.
- Yoo, D.Y., Kwon, K.Y., Park, J.J. and Yoon, Y.S. (2015), "Local bond-slip response of GFRP rebar in ultra-high-performance fiber-reinforced concrete", *Compos. Struct.*, **120**(2), 53-64. <https://doi.org/10.1016/j.compstruct.2014.09.055>.
- Zhang, S.H., Shao, X.D., Cao, J.H., Cui, J.F., Hu, J.H. and Deng, L. (2016), "Fatigue performance of a lightweight composite bridge deck with open ribs", *J. Bridge. Eng.*, **21**(7), 04016039. [https://doi.org/10.1061/\(ASCE\)BE.1943-5592.0000905](https://doi.org/10.1061/(ASCE)BE.1943-5592.0000905).

PL